Article:
Calvopina, K, Hinchliffe, P, Brem, J et al. (8 more authors) (2017) Structural/mechanistic insights into the efficacy of nonclassical β-lactamase inhibitors against extensively drug resistant Stenotrophomonas maltophilia clinical isolates. Molecular Microbiology, 106 (3). pp. 492-504. ISSN 0950-382X

https://doi.org/10.1111/mmi.13831

Structural and mechanistic studies reveal the effectiveness of non-classical β-lactamase inhibitors against extensively drug resistant Stenotrophomonas maltophilia.

Running Title: β-Lactamase inhibitors versus S. maltophilia.

Karina Calvopiña[1], Philip Hinchliffe[1], Jürgen Brem[2], Kate J. Heesom[3], Samar Johnson[1], Ricky Cain[4], Christopher T. Lohans[2], Colin W. G. Fishwick[4], Christopher J. Schofield[2], James Spencer[1], and Matthew B. Avison[1]*.

[1]School of Cellular & Molecular Medicine, University of Bristol, Bristol, United Kingdom.

[2]Department of Chemistry, University of Oxford, Oxford, United Kingdom.

[3]Bristol University Proteomics Facility, Bristol. United Kingdom.

[4] School of Chemistry, University of Leeds, Leeds. United Kingdom.

Correspondence to: School of Cellular & Molecular Medicine, University of Bristol, Biomedical Sciences Building, University Walk. Bristol BS81TD, United Kingdom.

bimba@bris.ac.uk.

Word count for the abstract: 175

Word count for the text: 5498

ABSTRACT

Clavulanic acid and avibactam are clinically deployed serine β-lactamase inhibitors, important as a defence against antibacterial resistance. Bicyclic boronates are recently discovered inhibitors of serine and some metallo-β-lactamases. Here were show that avibactam and a bicyclic boronate inhibit L2 (serine β-lactamase) but not L1 (metallo β-lactamase) from the extensively drug resistant human pathogen Stenotrophomonas maltophilia. Both inhibitors bind L2 by covalent attachment to the nucleophilic serine and reverse ceftazidime resistance in S. maltophilia because, unlike clavulanic acid, they do not induce L1 production. Ceftazidime/inhibitor resistant mutants hyperproduce L1, but retain aztreonam/inhibitor susceptibility because aztreonam is not an L1 substrate. Importantly, avibactam, but not the bicyclic boronate is deactivated by L1 at a low rate; the utility of avibactam might be compromised by mutations that increase this deactivation rate. These data rationalize the observed clinical efficacy of ceftazidime/avibactam plus aztreonam as combination therapy for S. maltophilia infections and confirm that aztreonam-like β-lactams plus non-classical β-lactamase inhibitors, particularly avibactam-like and bicyclic boronate compounds, have potential for treating infections caused by this most intractable of drug resistant pathogens.

IMPORTANCE

Stenotrophomonas maltophilia is an important bacterial pathogen that causes severe infections in immunocompromised and debilitated patients. It can become resistant to all β-lactam antibacterials via mutations that enhance L1 and L2 β-lactamase production. Using steady state enzyme kinetics, x-ray crystallography and NMR spectroscopy, we characterised the interactions of various β-lactamase inhibitors with L1 and L2. These findings, together with whole cell susceptibility tests and proteomic analysis of resistant mutants explained why aztreonam plus the clinically available non-β-lactam based β-lactamase inhibitor avibactam is an excellent combination against S. maltophilia, rationalising its recently confirmed clinical effectiveness. We also showed that despite its very different chemical structure, a cyclic boronate that is currently in development matches avibactam as an L2 inhibitor and in its ability to reverse β-lactam resistance in S. maltophilia but it is potentially superior because, unlike avibactam, it is not susceptible to breakdown by L1.

INTRODUCTION

β-Lactamases are the most commonly encountered cause of resistance to β-lactams, which are the most frequently prescribed class of antibacterial drug world-wide (1-3). β-Lactamases render β-lactams inactive through catalysing efficient hydrolysis of the β-lactam ring (4, 5). There are many hundreds of β-lactamases, which are grouped based on sequence and mechanism into the serine β-lactamase (SBL) classes A, C and D, and the metallo-β-lactamase (MBL) subclasses B1, B2 and B3) (6, 7). Broad-spectrum, clinically useful β-lactamase inhibitors are being sought, but the varying chemistries and active site architectures of the different β-lactamase classes makes the development of cross-class inhibitors extremely challenging (8-10).

Clavulanic acid (**Fig. 1, top**) is a well-established clinically deployed β-lactam-based inhibitor of, principally, class A SBLs. Clavulanic acid is used in combination with penicillin derivatives such as amoxicillin and ticarcillin, whose bactericidal effects improve against some β-lactamase-carrying isolates of species such as Escherichia coli and Klebsiella pneumoniae (11-14). Clavulanic acid is an irreversible inhibitor of class A enzymes, whose activity arises from fragmentation of the acyl-enzyme complex formed by reaction with the active-site serine nucleophile, to generate a near permanently inactivated species (15). In contrast, avibactam, a recently introduced relatively broad spectrum non-β-lactam-based SBL inhibitor contains a diazobicyclo heterocyclic core structure which reversibly acylates SBLs. The potency of avibactam against class A, C and some class D SBLs is attributed to the stabilization of the carbamoyl complex due to interactions with polar residues present in the active sites, with de-acylation preferentially occurring due to recyclization rather than hydrolytic turnover (16). This results in release of intact active inhibitor rather than an inactive hydrolysis product (**Fig. 1, middle**) (17-20). Avibactam has recently been licenced for clinical use in partnership with the

78 oxy-amino cephalosporin ceftazidime, though the combination is not universally efficacious
79 and has no useful activity against MBL-producing bacteria (18, 21).

80 Boronic acid-based compounds have long been studied as potential SBL inhibitors but,
81 in most cases, are ineffective against MBL targets. For example, the monocyclic boronate,
82 RPX7009, which is in phase 3 clinical trials, is effective against Class A, C and D β-lactamases,
83 but not MBLs (22). However, we recently demonstrated that bicyclic boronate scaffolds can
84 act as potent inhibitors of multiple SBL classes as well as subclass B1 MBLs (9). Accordingly,
85 one method of overcoming the poor activity of ceftazidime/avibactam against MBL producing
86 bacteria would be to combine ceftazidime with a bicyclic boronate inhibitor, such as **2** (**Fig. 1,**
87 **bottom**), which represents the closest approach to pan-β-lactamase inhibitor that has, to-date,
88 been reported (23). One bicyclic boronate is currently in phase 1 clinical trials (24)

89 Stenotrophomonas maltophilia (25) is one of the most intrinsically multidrug resistant
90 bacterial species encountered in the clinic. It causes serious infections with high mortality rates
91 in immunocompromised and severely debilitated patients, and colonises the lungs of 30% of
92 patients with cystic fibrosis (26, 27). While S. maltophilia possesses multiple efflux systems
93 (28-31) that reduce the net rate of entry for many antimicrobials, β-lactam resistance arises
94 primarily from production of two β-lactamases, a subclass B3 MBL "L1", which hydrolyses
95 all β-lactams except for the monobactam, aztreonam, and the class A Extended Spectrum SBL
96 (ESBL) "L2", which hydrolyses all first to third generation cephalosporins, all penicillins, and
97 aztreonam (32-34). The combination of L1 and L2, therefore renders S. maltophilia resistant
98 to all β-lactam antibiotics although in clinical practice, ceftazidime can be useful, because most
99 clinical isolates do not produce enough β-lactamase to give resistance (35, 36). Ceftazidime
100 resistant mutants rapidly emerge through hyper-production of L1 and L2, via single site
101 mutations either in the L1/L2 transcriptional activator, ampR, or in several possible genes

whose products influence AmpR (36, 37). Accordingly, S. maltophilia represents one of the most challenging targets for β-lactam/β-lactamase inhibitor combinations.

Here we report kinetic and structural studies with purified S. maltophilia β-lactamases, in vitro testing of various β-lactam/β-lactamase inhibitor combinations against extensively drug resistant clinical S. maltophilia isolates, and characterisation of acquired resistance to these combinations. The results reveal that non-classical β-lactamase inhibitors such as avibactam and bicyclic boronates have considerable potential in combatting β-lactam resistance in S. maltophilia, particularly when put in combination with aztreonam-like β-lactams.

RESULTS

β-lactamase inhibitors restore aztreonam, but not meropenem activity against S. maltophilia

As a prelude to investigating the effects of β-lactamase inhibitors, we first evaluated the hydrolysis of a range of candidate β-lactams in vitro by purified L1 (subclass B3 MBL) and L2 (class A ESBL) under steady state conditions. These data (**Table 1**) reveal the carbapenem meropenem to be predominantly a substrate for L1, with L2 showing only weak hydrolytic activity, the monobactam aztreonam to be a substrate for L2 only, and that both L1 and L2 can hydrolyse the oxyamino-cephalosporin ceftazidime with similar efficiencies.

We next tested the ability of three β-lactamase inhibitors: clavulanic acid, avibactam and the bicyclic boronate **2** (each at 2 mg/L) to potentiate the activity of the target β-lactams against S. maltophilia (**Table 2**) All three inhibitors reversed aztreonam, but not meropenem resistance in ceftazidime susceptible clinical isolates (K279a, CI-20, CI-29). Furthermore, all three inhibitors reversed ceftazidime and aztreonam, but not meropenem, resistance in a ceftazidime-resistant L1/L2 hyper-producing mutant (K CAZ 10), derived from K279a (**Table 2**) (37). However, all three inhibitors failed to restore ceftazidime susceptibility in a ceftazidime

resistant L1/L2 hyper-producing clinical isolate (CI-31). Importantly, there is no general block on inhibitor activity in CI-31, as all three inhibitors could reverse aztreonam resistance in this isolate (**Table 2**).

Efflux pumps play a major role in antimicrobial resistance in S. maltophilia (26, 38). Thus, to investigate the possible effect of multi-drug efflux pumps on β-lactamase inhibitor efficacy, we selected two hyper-resistant mutants from the isolate K279a using moxifloxacin and amikacin, known to be efflux pump substrates. Comparative proteomics (**Tables S1, S2, Fig. 2**) confirmed that the two mutants, K MOX 8 and K AMI 32, hyper-produce the SmeDEF and SmeYZ efflux pumps, respectively. In K MOX 8, SmeYZ was downregulated as SmeDEF was hyperproduced, as expected given their reciprocal regulation (39)]. All three β-lactamase inhibitors retained full activity against these efflux pump hyperproducing mutants (**Table 2**) ruling out efflux as a contributing factor to the observed variation in efficacy of the various β-lactam/β-lactamase inhibitor combinations.

The bicyclic boronate 2 does not inhibit the S. maltophilia L1 MBL

Based on these in vitro data we conclude that the bicyclic boronate **2** acts against S. maltophilia in a similar fashion to avibactam and clavulanic acid: it reverses aztreonam and, when due to L1/L2 hyperproduction, ceftazidime resistance (**Table 2**). As **2** has been shown to inhibit multiple MBLs (9), we anticipated that it might also inhibit L1, but the fact that **2** does not reverse resistance to meropenem (**Table 2**), which is predominantly hydrolysed by L1 (**Table 1**) suggests that this is not the case.

As, to date, the inhibition of subclass B3 MBLs by bicyclic boronates has not been reported, we investigated the inhibition of purified L1 and L2 by the three β-lactamase inhibitors using the fluorogenic β-lactamase substrate FC5 as a new reporter for L1 and

L2(40). Steady-state k_{cat}/K_M values clearly demonstrate that FC5 is hydrolysed with a higher efficiency than other β-lactams by both L1 and L2 (**Table 1**). IC_{50} measurements revealed that while all three β-lactamase inhibitors inhibit L2 with nanomolar potencies (**Table 3**), no inhibition of L1 was observed, even when using inhibitor concentrations up to 2.5 mM. NMR spectroscopy confirmed that there is no impact of avibactam or **2** on meropenem hydrolysis by L1 (**Fig 3A**). NMR experiments also showed that L1 can hydrolyse avibactam, albeit at a slow rate, but it does not modify **2** to any detectable extent following incubation up to 24 h (**Fig. 3B,C**). Thus, unlike the case for subclass B1 MBLs (9), the bicyclic boronate **2** is not an effective inhibitor of the subclass B3 MBL L1.

Structural basis for inhibition of L2 by avibactam and the bicyclic boronate 2

The results above demonstrate that, consistent with the effectiveness of β-lactam/β-lactamase inhibitor combinations against S. maltophilia strains, L2 is effectively inhibited by both avibactam and the bicyclic boronate **2**. To investigate the molecular basis for this inhibition we crystallised L2 and soaked the crystals in avibactam or **2**. Consistent with our inhibition kinetics results, we were unable to obtain crystal structures of complexes of L1 with either of these inhibitors. L2 crystallised in the space group $P2_12_12_1$ with two molecules in the asymmetric unit (**Table S3**), and closely conserves the overall SBL fold with, for example, an RMSD to KPC-2 (PDB 2OV5) of 0.2 Å. L2 crystals formed in a reagent containing a racemic mixture of the amino acids glutamate, alanine, lysine and serine. The active site manifests clear F_o-F_c density into which a molecule of D-glutamate could be modelled (**Fig 4A**), indicating the D-enantiomer preferentially binds to L2. However, binding does not perturb the active site conformation compared with an un-complexed L2 crystal structure (PDB 1O7E) (**Fig S1**), preserving positioning of the hydrolytic (deacylating) water with respect to Glu166, Asn170

and Ser70 (see **Table S4** for distances), and the conformation of the conserved, catalytically important Lys73 (41-43) . D-glutamate binds non-covalently, through interactions of its carbonyl oxygen with the backbone amides in the oxyanion hole (formed by residues Ser70 and Ser237), the C-terminal oxygen with Ser130-Oγ, and the glutamate amide with the deacylating water (**Fig. 5A**). Despite these extensive interactions, there is little inhibitory effect, with 100 mM D-glutamate reducing L2 activity by just 21% +/- 2% (Mean +/- Standard Deviation n=4). D-glutamate binds differently compared with the high affinity binding (K_i = 84 pM) of the β-lactamase inhibitory protein (BLIP) to the class A β-lactamase KPC-2 (PDB 3E2K). Interestingly, BLIP binding to KPC-2 involves localisations of an L-glutamate residues at the active site, in a manner related to, but different from, D-glutamate binding to L2, and one that does not involve interactions with the oxyanion hole (**Fig. S2**) (44).

L2:avibactam and L2:bicyclic boronate **2** co-complex structures were solved to 1.35 Å and 2.09 Å resolution, respectively, with clear F_o-F_c density indicating both inhibitors react with to the active site nucleophile Ser70 (**Figs 4B and 4C**). Binding by both compounds reveals no significant changes in the L2 active site in comparison with the apo or D-glutamate structures. Indeed, in both structures the deacylating water is positioned similarly to the native and D-glutamate-bound structures (**Table S4**).

The bicyclic boronate **2** binds L2 (**Figure 5B**) with the boron atom clearly in a tetrahedral geometry, as observed previously on binding of the cyclic boronate **1** to CTX-M-15 (another class A ESBL) (23) and OXA-10 (a class D SBL) (9), mimicking the first tetrahedral intermediate formed during β-lactam hydrolysis. As in D-glutamate binding, the assigned OH group on the boron atom is positioned to make strong interactions with the backbone amides of Ser70 (2.95 Å) and Ser237 (3.1 Å) in the oxyanion hole. The bicyclic boronate **2** makes additional hydrogen bonds to the side chains of the catalytically important residues Ser130 (2.77 Å to the bicyclic ring oxygen), Asn132 (3.0 Å to the acetamide oxygen),

Ser237 (2.96 Å to the carboxylate) Thr235 (2.65 Å to the carboxylate), and the backbone carbonyl oxygen of Ser237 (3.1 Å to the acetamide nitrogen). In addition, binding is stabilised by significant hydrophobic interactions with His105.

Avibactam (**Figure 5C**) binds to L2 in its ring opened form, forming a carbamoyl-enzyme complex (16) in which its six-membered ring is in a chair conformation, a conserved feature in other structurally characterised avibactam:β-lactamase complexes (45-50). Highlighting the importance of the oxyanion hole, as with both D-glutamate and the bicyclic boronate **2**, the avibactam derived carbamoyl oxygen is positioned to make hydrogen bonds with the oxyanion hole backbone amides of Ser70 (2.75 Å) and Ser237 (2.85 Å). His105 is also involved in providing stabilising hydrophobic interactions (3.49 Å), while the carbamoyl NH interacts with the backbone carbonyl of Ser237 (3.08 Å) and the Asn132 sidechain (2.97 Å). The carbamoyl NH interactions may be relatively less important as they present in only one molecule in the asymmetric unit (chain B). The avibactam sulfate moiety interacts with the OH groups of both Thr235 (3.10 Å) and Ser130 (2.88 Å), with an additional 3.19 Å interaction with Ser237 in chain B.

β-Lactamase production is not induced by avibactam and the bicyclic boronate 2

One important consideration when deploying β-lactamase inhibitors into clinical practice is that some can interact with penicillin binding proteins and trigger β-lactamase induction pathways carried by many bacteria. L1 and L2 production in S. maltophilia is controlled by a transcriptional regulator, AmpR, which is responsive to β-lactam challenge via sensing β-lactam mediated perturbations in peptidoglycan breakdown and recycling (51, 52). Hence, we tested the ability of β-lactamase inhibitors to induce β-lactamase production in S. maltophilia. Clavulanic acid induces L1 production (measured using meropenem hydrolysis in cell extracts)

223 at a similar level to the positive control β-lactam cefoxitin in the S. maltophilia wild type strain
224 K279a (**Fig. 6**). This rationalizes why clavulanic acid does not reduce the MIC of ceftazidime
225 against S. maltophilia K279a (**Table 2**): induction of L1 (**Fig. 6**) overcomes inhibition of L2
226 (**Table 3**) because L1 can hydrolyse ceftazidime (**Table 1**). Since L1 does not hydrolyse
227 aztreonam (**Table 1**), however, clavulanic acid reduces the aztreonam MIC against K279a,
228 despite its ability to induce L1 production (**Table 2, Fig. 6**). Notably, by contrast with
229 clavulanic acid, both avibactam and the bicyclic boronate **2** reduce ceftazidime MICs against
230 K279a (**Table 2**). This observation is explained by the important finding that neither avibactam
231 nor **2** induces L1 to any measurable extent (**Fig. 6**), yet both inhibit L2 (**Table 3**).

232

233 **Selection and characterisation of mutants which overcome the reversal of ceftazidime**
234 **resistance by avibactam and the bicyclic boronate 2.**

235 Avibactam is currently only clinically available in combination with ceftazidime. The fact that
236 L1 induction by clavulanic acid overcomes its ability to reduce ceftazidime MICs against S.
237 maltophilia (**Fig. 6, Table 2**) led us to suggest that L1/L2 hyper-producing, ceftazidime
238 resistant strains might further mutate to be ceftazidime resistant in the presence of avibactam
239 and the bicyclic boronate **2** by producing even more L1. To investigate this possibility, we used
240 a K279a ampR mutant, M11, which is ceftazidime resistant due to L1/L2 hyperproduction but
241 where ceftazidime resistance can be reversed following treatment with avibactam or **2** at 10
242 mg/L (**Table 4**). We aimed to identify mutants able to grow on ceftazidime at >32 mg/L (i.e.
243 clinically resistant, according to CLSI breakpoints (53) in the presence of either avibactam or
244 **2** at 10 mg/L. Mutants were readily obtained; those selected using ceftazidime/avibactam were
245 also resistant to ceftazidime/**2**, and vice versa (**Table 4**). To investigate the basis for this
246 resistance, LC-MS/MS proteomics was used to quantify changes in protein production in the

two mutants. In both cases, L1 was produced at levels ~3-fold greater than in the parent strain (**Table S5, S6, Fig. 7A**). This result was confirmed by measuring L1 enzyme activity in cell extracts using meropenem as substrate (**Fig 7B**). Thus, hyperproduction of L1 can overcome the ability of these L2-specific inhibitors to rescue ceftazidime activity against a ceftazidime-resistant strain. Importantly, however, the mutants were still sensitive to the aztreonam/avibactam or aztreonam/**2** combinations (**Table 4**) as L1 cannot hydrolyse aztreonam (**Table 1**). This L1 hyperproducing phenotype, blocking reversal of ceftazidime, but not aztreonam, resistance by β-lactamase inhibitors is clearly relevant, because it is displayed by clinical isolate CI-31 (**Table 2**).

DISCUSSION

Our structural data reveal that avibactam and bicyclic boronates bind to L2 in a manner similar to those previously observed for other class A SBLs. For the bicyclic boronate **2**, binding of the tetrahedral boron atom to L2 and conformation of the bicyclic fused core are all consistent with the CTX-M-15:bicyclic boronate **1** structure (23); there is only slight variation in the amide/aromatic acetamide side chain conformations (**Fig. 8A**). Formation of the L2 carbamoyl-enzyme complex by avibactam results in a conformationally similar mode of binding compared with the structurally-characterised complexes with the class A SBLs KPC-2 (PDB 4ZBE) (45), SHV-1 (PDB 4ZAM) (45) and CTX-M-15 (PDB 4S2I) (46) (**Fig. 8B**), and is consistent with data indicating avibactam to be similarly effective against these enzymes (16, 45, 54). However, some subtle differences in active-site interactions are observed (**Fig S3**). In particular, while the avibactam carbamoyl hydrogen bond with Asn132 is conserved, the weaker carbamoyl interaction with the carbonyl oxygen of L2-Ser237 is not, highlighting that this is not essential for binding. Furthermore, the avibactam sulfate moiety interaction with

Thr235 is likely important as it presents in all SBLs, while interaction with Ser130 is present in KPC-2 alone. In SHV-1:avibactam, interaction of the sulfate group with the non-conserved Arg244 essentially substitutes for the sulfate-Ser237 interaction in other SBLs (Thr237 in KPC-2). In both SHV-1:avibactam and KPC-2:avibactam the 'hydrolytic' deacylating water molecule hydrogen bonds to the avibactam carbamoyl, while this is not observed with either CTX-M-15:avibactam or L2:avibactam. The avibactam-derived sulfate-bonded nitrogen is in the same conformation as in KPC-2/SHV-1:avibactam and, unlike in the CTX-M-15:avibactam complex, is directed away from the six-membered ring and distant from Ser130 (Ser130, 3.57 Å) (46) and consequently is not primed for re-cyclization (20) in which this residue is involved (**Fig. 8B**). The CTX-M-15:avibactam complex therefore remains to date as the only crystallographic evidence for avibactam reacting with an SBL in a conformation ideal for re-cyclization (46). Thus, the degree to which the avibactam derived complex can re-cyclize to reform intact avibactam may vary between SBLs.

Even though our structural and kinetic work confirm that L2 is potently inhibited by avibactam and the bicyclic boronate **2**, we predicted failure of avibactam/ceftazidime against S. maltophilia. This is because mutants that hyperproduce L1 are readily obtained from S. maltophilia isolates (**Fig. 7**), and avibactam does not inhibit MBLs (21). Whilst **2** inhibits subclass B1 MBLs (9), our work reveals that it does not inhibit the subclass B3 MBL, L1 (**Table 3**) and so **2**/ceftazidime was also overcome by L1 hyperproduction (**Table 4, S5, S6, Fig. 7**). It may be possible to modify **2** and so generate a broader-spectrum MBL inhibitor. However, a key finding of this work is that such a modification might not be essential. Avibactam and **2** both facilitate killing of S. maltophilia when paired with the monobactam, aztreonam, reducing MICs to ≤ 4 mg/L even in the pan-resistant clinical S. maltophilia isolate, CI-31 (**Table 2**). This implies that aztreonam/avibactam and aztreonam/**2** may have a promising clinical future for treatment of infections caused by this most intractable of species.

296 The fact that efflux pump overproduction does not affect aztreonam/**2** or aztreonam/avibactam
297 activity (**Table 2**) gives even greater cause for optimism. We were interested to read, therefore,
298 a recent clinical case report demonstrating the use of combination therapy with
299 ceftazidime/avibactam plus aztreonam to save the life of a patient with an S. maltophilia
300 infection that had failed all prior therapy (55) . Our structural, kinetic and whole bacterial
301 killing data would lead to the conclusion that ceftazidime was probably superfluous in this
302 success, but our work indicates that ceftazidime/avibactam plus aztreonam might be routinely
303 considered in the clinic for use against seemingly untreatable S. maltophilia infections whilst
304 aztreonam/avibactam works its way through the clinical trials system.

305 In many respects, because of its inability to inhibit L1, the bicyclic boronate **2** acts
306 against S. maltophilia very similarly to avibactam. One potentially significant difference is that
307 avibactam, but not **2**, is hydrolysed by L1 (**Fig. 3**). This hydrolysis is slow, and even if L1 is
308 hyperproduced, it is not significant enough to confer aztreonam/avibactam resistance (**Table**
309 **4**). However, there is a chance that L1 mutants might be selected with greater avibactam
310 hydrolytic activity, reducing the degree of L2 inhibition and raising the MIC of
311 aztreonam/avibactam into the resistant range. This may also be of relevance to other avibactam-
312 like compounds in development, e.g. Relebactam (56). In contrast, given that hydrolysis of **2**
313 by wild-type L1 is undetectably slow, evolution to increased breakdown may require
314 significantly more steps, potentially increasing the long-term efficacy of aztreonam/**2** as a
315 combination to treat S. maltophilia infections.

316 In conclusion, our combined results reveal the potential of non-classical non β-lactam
317 containing β-lactamase inhibitors, including the clinically approved compound avibactam, and
318 the cyclic boronates (some of which are presently in clinical trials) for treatment of S.
319 maltophilia, particularly when partnered with the monobactam aztreonam, and perhaps other
320 aztreonam-like β-lactams currently in development Given, the structural differences, between

avibactam, cyclic boronates, and the β-lactam based inhibitors, it would seem that there is considerable scope for the identification of new types of β-lactamase inhibitors of potential clinical utility against Gram-negative bacterial pathogens.

MATERIALS AND METHODS

Bacterial isolates and materials

S. maltophilia clinical isolates were K279a, a well characterised isolate from Bristol, UK, or were obtained from the SENTRY antimicrobial resistance survey, as previously reported (37). The ceftazidime resistant, β-lactamase hyper-producing mutant K CAZ 10 has previously been described [34]. Efflux-pump over producing mutants K AMI 32 and K MOX 8 were selected using K279a as parent strain as described previously (29). All growth media were from Oxoid. Chemicals were from Sigma, unless otherwise stated. Avibactam was from AstraZeneca whilst cyclic boronate **2** was synthesised according to published protocols (57).

Assay of β-lactamase activity in cell extracts, β-lactamase induction and β-lactam susceptibility

Cultures were grown overnight using nutrient broth and used to inoculate (1:100 dilution) 10 mL nutrient broth cultures in sealed 30 mL universal bottles. Cultures were incubated for 2 h with shaking at 37°C before test inducers were added, or not, and culture was continued for 2 h. Cells were pelleted by centrifugation (4,000 x g, 10 min) and pellets treated with 100 µL of BugBuster (Ambion), pipetting up and down a few times before rocking for 10 min at room temperature. Cell debris and unlysed cells were pelleted by centrifugation (13,000 x g, 5 min) and the supernatant retained as a source of crude cell protein. Protein concentrations were

determined using the BioRad protein assay reagent concentrate according to the manufacturer's instructions. L1 β-lactamase activity was determined using an Omega Fluostar (BMG Biotech) using meropenem as substrate in half-area 96 well UV-translucent plates (Greiner UV-Star. Bio-one) with 200 µL of 100 µM meropenem solution in assay buffer (60 mM $Na_2HPO_4 \cdot 7H_2O$ pH 7.0, 40 mM $NaH_2PO_4 \cdot H_2O$, 10 mM KCl, 1 mM $MgSO_4 \cdot 7H_2O$, 100 µM $ZnCl_2$) plus 10 µL of cell extract. Substrate depletion was followed at 300 nm for 10 mins and an extinction coefficient of 9600 AU/M was used to calculate enzyme activity in the linear phase of the reaction.

Susceptibility to β-lactams in bacterial isolates was determined using the CLSI microtitre MIC methodology with Muller-Hinton Broth using 96 well plates (Corning, Costar). The MIC was determined as the lowest concentration of β-lactam required to entirely suppress growth (53). Inhibitor concentrations were kept constant at 2 mg/L or 10 mg/L in all assays. Interpretation of susceptibility/resistance was by reference to CLSI clinical breakpoints for S. maltophilia (ceftazidime) and for Pseudomonas aeruginosa (for aztreonam and meropenem, since no S. maltophilia breakpoints are available) (53).

Proteomic Analysis

Cells in 50 mL nutrient broth cultures were pelleted by centrifugation (10 min, 4,000 × g, 4˚C) and resuspended in 20 mL of 30 mM Tris-HCl, pH 8 and broken by sonication using a cycle of 1 sec on, 0.5 sec off for 3 min at amplitude of 63% using a Sonics Vibracell VC-505TM (Sonics and Materials Inc., Newton, Connecticut, USA). The sonicated samples were centrifuged at 8,000 rpm (Sorval RC5B PLUS using an SS-34 rotor) for 15 min at 4˚C to pellet intact cells and large cell debris; the supernatant was removed and concentrated (Amicon 3 kDa cutoff filter) for analysis of total cell protein. Alternatively, for envelope preparations, the

supernatant was not concentrated, and instead, subjected to centrifugation at 20,000 rpm for 60 min at 4˚C using the above rotor to pellet total envelopes. To isolate total envelope proteins, this total envelope pellet was solubilised using 200 µL of 30 mM Tris-HCl pH 8 containing 0.5% (w/v) SDS.

Protein concentrations in all samples was quantified using Biorad Protein Assay Dye Reagent Concentrate according to the manufacturer's instructions. Proteins (2.5 µg/lane for total cell proteomics or 5 µg/lane for envelope protein analysis) were separated by SDS-PAGE using 11% acrylamide, 0.5% bis-acrylamide (Biorad) gels and a Biorad Min-Protein Tetracell chamber model 3000X1. Gels were resolved at 200 V until the dye front had moved approximately 1 cm into the separating gel. Proteins in all gels were stained with Instant Blue (Expedeon) for 20 min and de-stained in water.

The 1 cm of gel lane was subjected to in-gel tryptic digestion using a DigestPro automated digestion unit (Intavis Ltd). The resulting peptides from each gel fragment were fractionated separately using an Ultimate 3000 nanoHPLC system in line with an LTQ-Orbitrap Velos mass spectrometer (Thermo Scientific). In brief, peptides in 1% (v/v) formic acid were injected onto an Acclaim PepMap C18 nano-trap column (Thermo Scientific). After washing with 0.5% (v/v) acetonitrile plus 0.1% (v/v) formic acid, peptides were resolved on a 250 mm × 75 µm Acclaim PepMap C18 reverse phase analytical column (Thermo Scientific) over a 150 min organic gradient, using 7 gradient segments (1-6% solvent B over 1 min., 6-15% B over 58 min., 15-32% B over 58 min., 32-40% B over 5 min., 40-90% B over 1 min., held at 90% B for 6 min and then reduced to 1% B over 1 min.) with a flow rate of 300 nL/min. Solvent A was 0.1% formic acid and Solvent B was aqueous 80% acetonitrile in 0.1% formic acid. Peptides were ionized by nano-electrospray ionization MS at 2.1 kV using a stainless-steel emitter with an internal diameter of 30 µm (Thermo Scientific) and a capillary temperature of 250°C. Tandem mass spectra were acquired using an LTQ-Orbitrap Velos mass

spectrometer controlled by Xcalibur 2.1 software (Thermo Scientific) and operated in data-dependent acquisition mode. The Orbitrap was set to analyze the survey scans at 60,000 resolution (at m/z 400) in the mass range m/z 300 to 2000 and the top twenty multiply charged ions in each duty cycle selected for MS/MS in the LTQ linear ion trap. Charge state filtering, where unassigned precursor ions were not selected for fragmentation, and dynamic exclusion (repeat count, 1; repeat duration, 30 s; exclusion list size, 500) were used. Fragmentation conditions in the LTQ were as follows: normalized collision energy, 40%; activation q, 0.25; activation time 10 ms; and minimum ion selection intensity, 500 counts.

The raw data files were processed and quantified using Proteome Discoverer software v1.4 (Thermo Scientific) and searched against the UniProt S. maltophilia strain K279a database (4365 protein entries; UniProt accession UP000008840) using the SEQUEST (Ver. 28 Rev. 13) algorithm. Peptide precursor mass tolerance was set at 10 ppm, and MS/MS tolerance was set at 0.8 Da. Search criteria included carbamidomethylation of cysteine (+57.0214) as a fixed modification and oxidation of methionine (+15.9949) as a variable modification. Searches were performed with full tryptic digestion and a maximum of 1 missed cleavage was allowed. The reverse database search option was enabled and all peptide data was filtered to satisfy false discovery rate (FDR) of 5 %. The Proteome Discoverer software generates a reverse "decoy" database from the same protein database used for the analysis and any peptides passing the initial filtering parameters that were derived from this decoy database are defined as false positive identifications. The minimum cross-correlation factor filter was readjusted for each individual charge state separately to optimally meet the predetermined target FDR of 5 % based on the number of random false positive matches from the reverse decoy database. Thus, each data set has its own passing parameters. Protein abundance measurements were calculated from peptide peak areas using the Top 3 method (58) and proteins with fewer than three peptides identified were excluded. The proteomic analysis was repeated three times for each parent and

mutant strain, each using a separate batch of cells. Data analysis was as follows: all raw protein abundance data were uploaded into Microsoft Excel. Raw data from each sample were normalised by division by the average abundance of all 30S and 50S ribosomal protein in that sample. A one-tailed, unpaired T-test was used to calculate the significance of any difference in normalised protein abundance data in the three sets of data from the parent strains versus the three sets of data from the mutant derivative. A p-value of <0.05 was considered significant. The fold change in abundance for each protein in the mutant compared to its parent was calculated using the averages of normalised protein abundance data for the three biological replicates for each strain. All raw protein abundance data are provided in the attached proteomics data file.

Purification of L1 and L2 and kinetics assays

Recombinant L1 and L2 proteins were produced in E. coli and purified as previously described (59). Enzyme activity was monitored using an Omega Fluostar (BMG Labtech) using buffer L1 (50 mM HEPES pH 7.5, 10 µg/mL BSA, 10 µM $ZnSO_4$ and 0.01% v/v Triton X-100) and buffer L2 (50 mM Tris pH 7.5, 10 µg/mL BSA and 0.01% v/v Triton X-100. Reactions were carried out as described in (40). For the chromogenic substrates meropenem, ceftazidime and aztreonam, substrate depletion was measured at 300 nm, 260 nm, 318 nm, respectively whilst for the fluorogenic substrate FC5, the excitation wavelength was set at 380nm and emission wavelength at 460 nm (40). Clavulanic acid was dissolved in double distilled water while avibactam and cyclic boronate **2** were dissolved in DMSO to prepare an appropriate stock solution. Steady state kinetic data were analysed by curve fitting to the Michaelis-Menten equation using Prism software.

L2 Crystallisation, Data Collection and Structure Modelling

Initial L2 crystals grew using sitting-drop vapour diffusion in 96-well MRC 2-drop plates (Molecular Dimensions) with the Morpheus sparse matrix screen (60). Conditions were refined in CrysChem 24-well sitting-drop plates (Hampton Research, 18 °C), and diffraction-quality crystals were obtained by mixing 1 µL of L2 protein (42 mg/mL) with 1.5 µL reagent (10% w/v PEG 20000, 20% v/v PEG MME 550, 0.02 M DL-Glutamic acid; 0.02 M DL-Alanine; 0.02 M Glycine; 0.02 M DL-Lysine; 0.02 M DL-Serine, 0.1 M bicine/Trizma base pH 8.5) and equilibrated against 500 µL reagent. L2 complexes were obtained by soaking crystals in bicyclic boronate **2** (5 min, 2.5 mM) or avibactam (40 min, 5 mM) dissolved in reservoir reagent. L2 crystals were cryoprotected using reservoir solution plus 20% glycerol and flash frozen in liquid nitrogen. Crystallographic data were collected at 100K (I04-1, I04 or I03, Diamond Light Source, UK) and integrated in XDS (61) or DIALS (62), and scaled in Aimless in the CCP4 suite (63). Phases were calculated by molecular replacement in Phaser (64) using PDB 1O7E (unpublished) as a starting model. Avibactam and boronate structures, covalently bound to Ser70, and geometric restraints were generated using Phenix eLBOW (65). Structures were completed by iterative rounds of manual model building in Coot (66) and refinement in Phenix (67). Structure validation was assisted by Molprobity (68) and Phenix (67). Figures were prepared using Pymol (Schrodinger).

NMR Spectroscopy

The potential impact of avibactam or the bicyclic boronate **2** (both 75 µM) on the hydrolysis of meropenem (1 mM) by L1 (75 nM) was monitored over 20 min. The hydrolysis of avibactam (400 µM) and **2** (400 µM) by L1 (10 µM) was monitored over the course of 18 h or 24 h,

respectively. All substrates, inhibitors, and enzymes were prepared in 50 mM Tris-d_{11}, pH 7.5, 10 % D_2O. Spectra were acquired on a Bruker AVIII 700 MHz spectrometer equipped with a $^{1}H/^{13}C/^{15}N$ TCI cryoprobe, and a Bruker AVIIIHD 600 MHz spectrometer equipped with a Prodigy broadband cryoprobe. ^{1}H spectra were acquired at 298 K using a 2 s relaxation delay, and were processed with a 0.3 Hz line broadening. The water signal was suppressed by excitation sculpting with perfect echo.

FUNDING INFORMATION

This work was funded, in part, by grants MR/N013646/1 to M.B.A & K.J.H, EP/M027546/1 to M.B.A & J.S and MR/N002679/1 to C.J.S. from the Antimicrobial Resistance Cross Council Initiative supported by the seven United Kingdom research councils. Additional funding was provided by grants from the National Institute of Allergy and Infectious Diseases of the U.S. National Institutes of Health (R01AI100560) to J.S and from the United Kingdom Medical Research Council and the Canadian Institute for Health Research (G1100135) to J.S. C.J.S. and C.W.G.F. K.C. was in receipt of a postgraduate scholarship from SENESCYT, Ecuador.

ACKNOWLEDGEMENTS

We thank Diamond Light Source for access to beamlines I03, I04 and I04-1 (proposal number MX12342) that contributed to the results presented here, and the staff of the Diamond macromolecular crystallography village for their help.

DATA AVAILABILITY

Coordinates and structure factors for L2:native, L2:avibactam and L2:cyclic boronate **2** have been deposited in the Protein Data Bank under accession codes 5NE2, 5NE3 and 5NE1, respectively.

AUTHOR CONTRIBUTIONS

Conception and design: MBA, JS, CJS, CGWF, PH, JB.

Acquisition of data: KC, PH, JB, KJH, SJ, RC, CTL.

Analysis and Interpretation of data: ALL AUTHORS.

Drafting the manuscript; ALL AUTHORS.

CONFLICTS OF INTEREST

NONE TO DECLARE (ALL AUTHORS)

FIGURE LEGENDS

Figure 1. Chemical structures of β-lactamase inhibitors.

Top, clavulanic acid. Middle, avibactam and the acyl-enzyme complex formed on the (potentially reversible) reaction of avibactam with SBLs. Bottom, bicyclic boronate **2**.

Figure 2. Efflux pump production in S. maltophilia mutants

Protein abundance data (relative to mean ribosomal protein Abundance for each sample) is reported as mean +/- Standard Error of the Mean (n=3). Full proteomics data are shown in Tables S1 and S2.

Figure 3. Interaction between Avibactam and Bicyclic Boronate 2 with L1 as measured by NMR Spectroscopy.

(A), impact of avibactam (75 μM) or bicyclic boronate **2** (75 μM) on the hydrolysis rate of meropenem (1 mM) as catlayzed by L1 (75 nM) in 50 mM Tris-d_{11}, pH 7.5, 10 % D_2O. (B) hydrolysis of avibactam (400 μM) as catalysed by L1 (10 μM), in 50 mM Tris-d_{11}, pH 7.5, 10 % D_2O. Signals corresponding to hydrolysed avibactam are indicated with asterisks (*). (C) Incubation of bicyclic boronate **2** (400 μM) for 24 h with and without L1 (10 μM), all in 50 mM Tris-d_{11}, pH 7.5, 10 % D_2O.

Figure 4. L2 active site views showing electron density maps calculated after removal of ligand.

F_o-F_c density (green, contoured at 3σ) calculated from the final model after removal of (A) D-glutamate, (B) bicyclic boronate **2** and (C) avibactam. Residues coordinating the 'deacylating' water (red sphere, 'Wat') are shown as sticks and labelled (Ser70, Glu166 and Asn170).

Figure 5. Interaction of β-lactamase inhibitors with the L2 active site.

View of L2 (shown in green cartoon) active sites with bound ligands (blue sticks), (A) D-glutamate, (B) bicyclic boronate **2** and (C) avibactam. Interactions between residues and the catalytic water are shown as red dashes, and interactions between residues and ligand as blue dashes. Labelled residues are those that specifically interact with the ligand.

Figure 6. L1 β-lactamase induction by β-lactamase inhibitors in S. maltophilia K279a.

S. maltophilia isolate K279a was incubated in presence of different potential inducers (cefoxitin, clavulanic acid, the bicyclic boronate 2, or avibactam) at 50 mg/L). L1 activity was measured from the cell extracts in a 96-well plate reader by determining meropenem hydrolysis (100 μM) at λ=300 nm. Protein concentration was determined by using the BioRad protein assay dye reagent. Specific activity was calculated by using the extinction coefficient of 9600 AU/M/cm and a pathlength correction for the microplate (0.62 mm). Data presented are means +/- SEM, n=3.

Figure 7. L1 activity of Inhibitor Resistant Mutants

In (A), L1 protein abundance data (relative to mean ribosomal protein abundance for each sample). Full proteomics data are shown in Tables S6 and S7. In (B), L1 enzyme activity in cell extracts is reported as meropenem hydrolysis rate. Data are reported as mean +/- SEM, n=3 for the parent strain, M11, and the two mutants (MA27 and MB25), which are resistant to ceftazidime/avibactam and ceftazidime/**2**.

Figure 8. Bicyclic boronate and avibactam binding conformations in Class A β-lactamases.

Superposition of inhibitors, shown as sticks, bound in the active sites of Class A β-lactamases. (A) Bicyclic boronates bound to L2 (blue, bicyclic boronate **2**) and CTX-M-15 (grey, bicyclic boronate **1**). (B) Avibactam bound to L2 (blue), SHV-1 (grey), KPC-2 (green) and CTX-M-15 (orange). Note the common binding mode for the bicyclic boronate bicyclic core and most of the avibactam structure; there are differences in the orientations of the avibactam core derived nitrogen (see text).

Supplemental figure 1. Comparison of the active sites of L2:D-glutamate with L2 native

L2:D-glutamate (green) and L2 native (PDB 1O7E, orange) are superposed and shown in cartoon, with important catalytic residues shown as sticks and the hydrolytic water (red) as a sphere.

Supplemental Figure 2. Superposition of L2:D-glutamate with KPC-2:BLIP.

The L2:D-glutamate structure is superposed with the crystal structure (PDB 3E2K) of BLIP (yellow) bound in the active site of KPC-2 (grey). Asp49 (stick, labelled) is the only BLIP residue making interactions in the KPC-2 active site, although binding is significantly different to D-glutamate (blue), with the exception of hydrogen bond formation to the side chains of S130 and T237 (labelled sticks; S237 in L2). Residues which interact with the catalytic water (red sphere) or form the oxyanion hole are labelled and shown as sticks.

Supplemental Figure 3. Comparisons of structurally characterised modes of binding of avibactam in class A SBLs.

Avibactam (grey sticks) is shown as complexed with L2 (blue, this study), SHV-1 (orange, PDB 4ZAM), KPC-2 (green, PDB 4ZBE), and CTX-M-15 (cyan, PDB 4S2I).

FIGURES

Figure 1

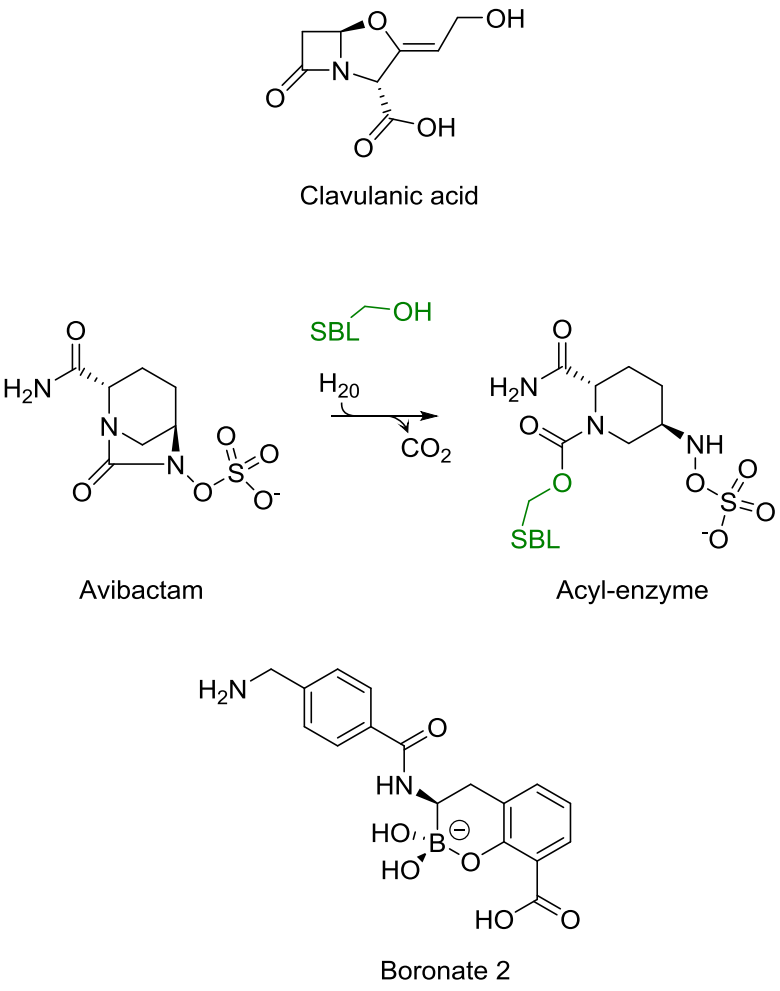

Figure 2

A

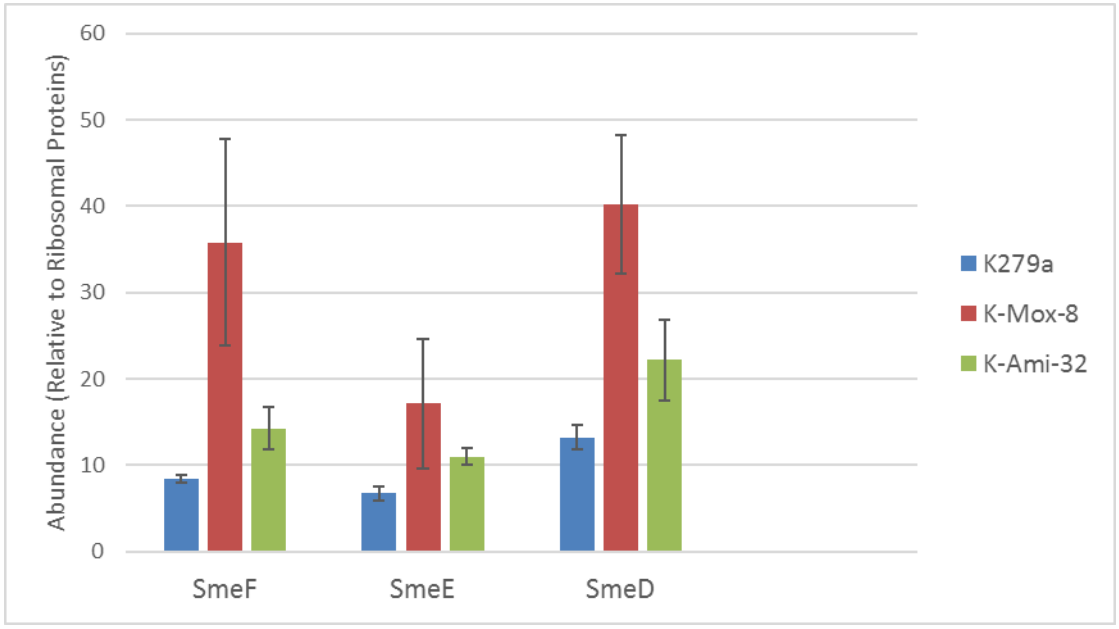
Abundance (Relative to Ribosomal Proteins)
60
50
40
30
20
10
0
SmeF
SmeE
SmeD
K279a
K-Mox-8
K-Ami-32

B

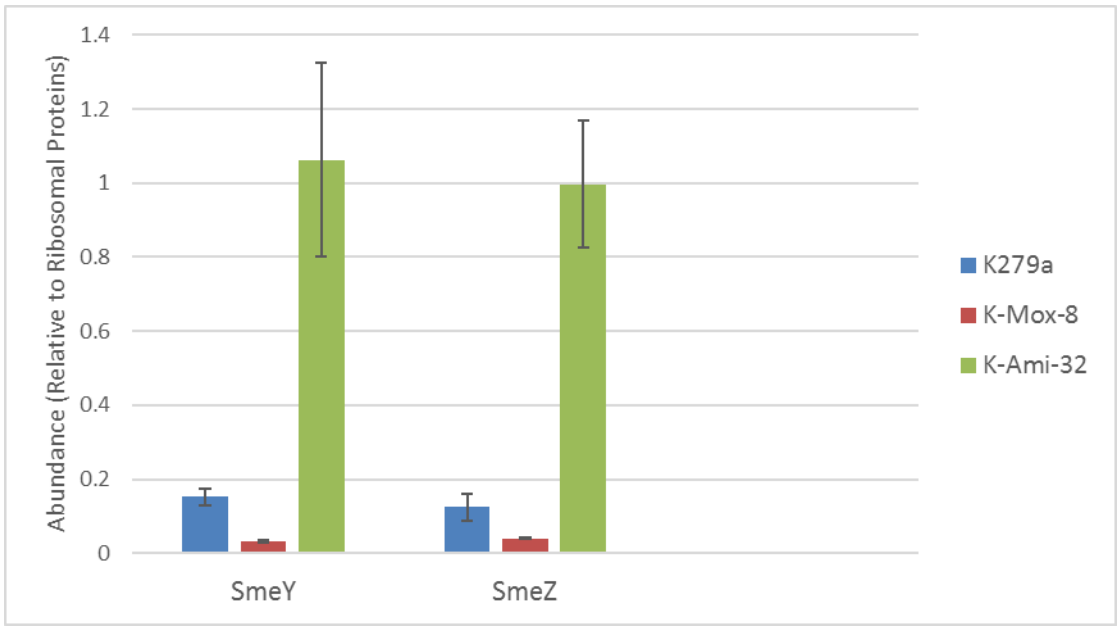
Abundance (Relative to Ribosomal Proteins)
1.4
1.2
1
0.8
0.6
0.4
0.2
0
SmeY
SmeZ
K279a
K-Mox-8
K-Ami-32

590 **Figure 3**

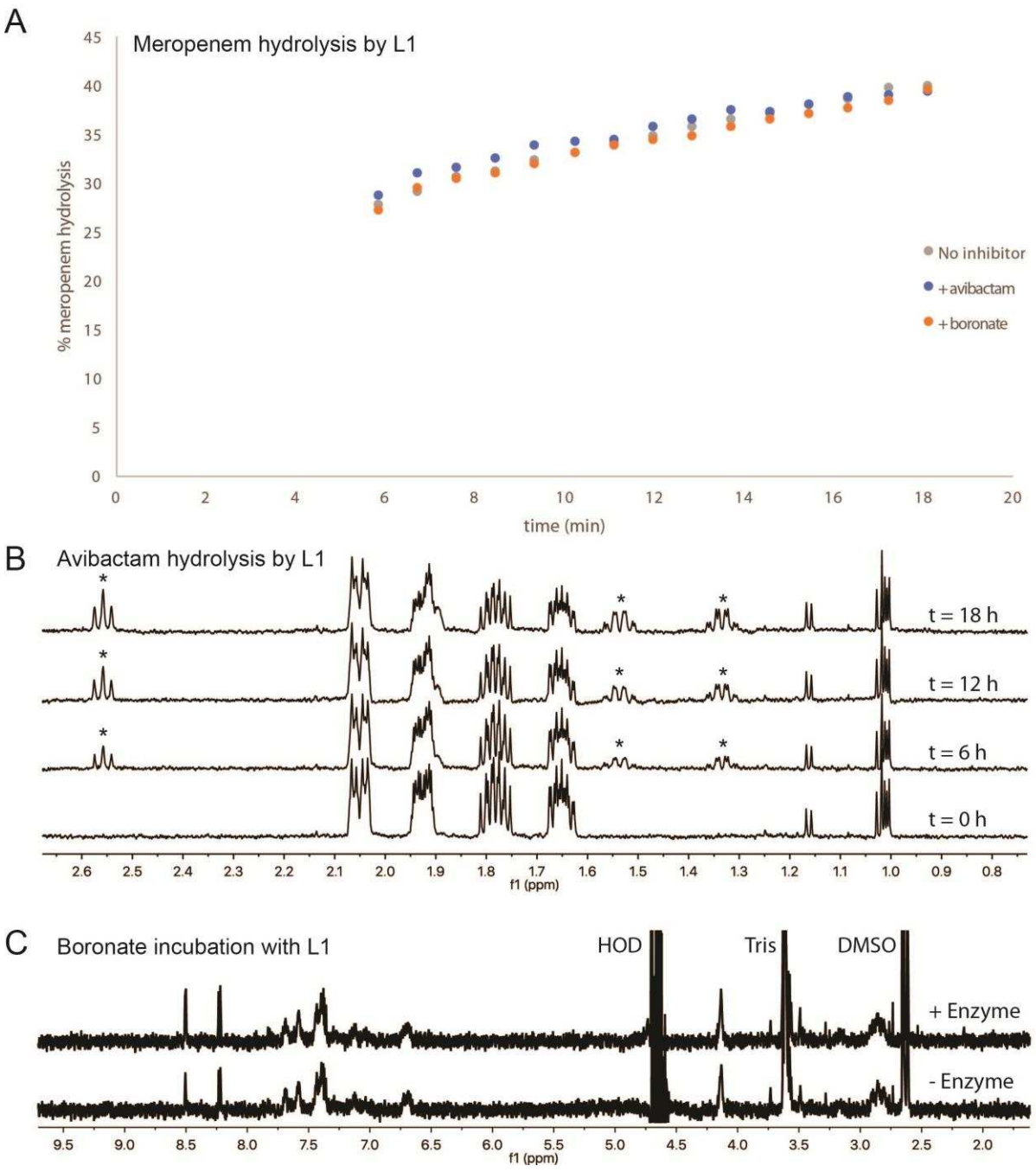

591

592

593 **Figure 4**

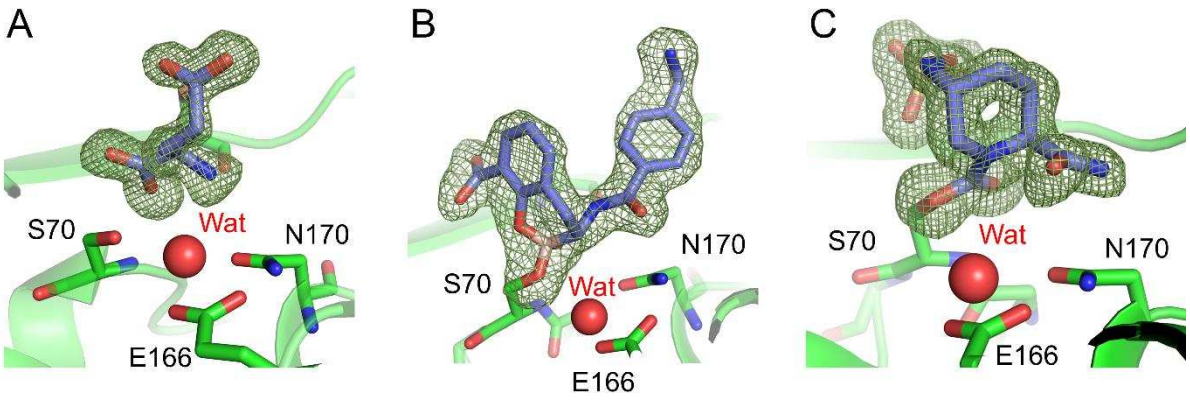

594

595 **Figure 5**

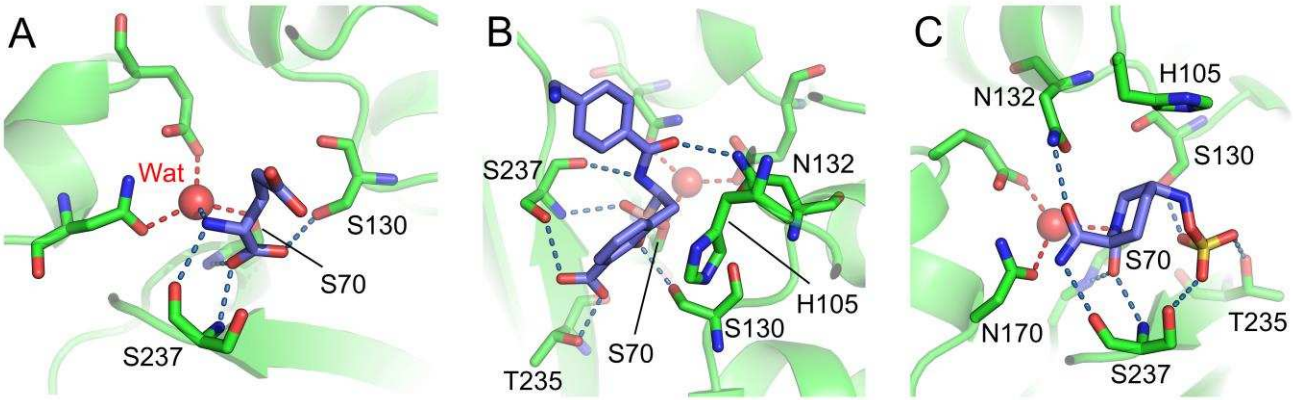

L2:*D*-glutamate L2:boronate 2 L2:avibactam

596

Figure 6

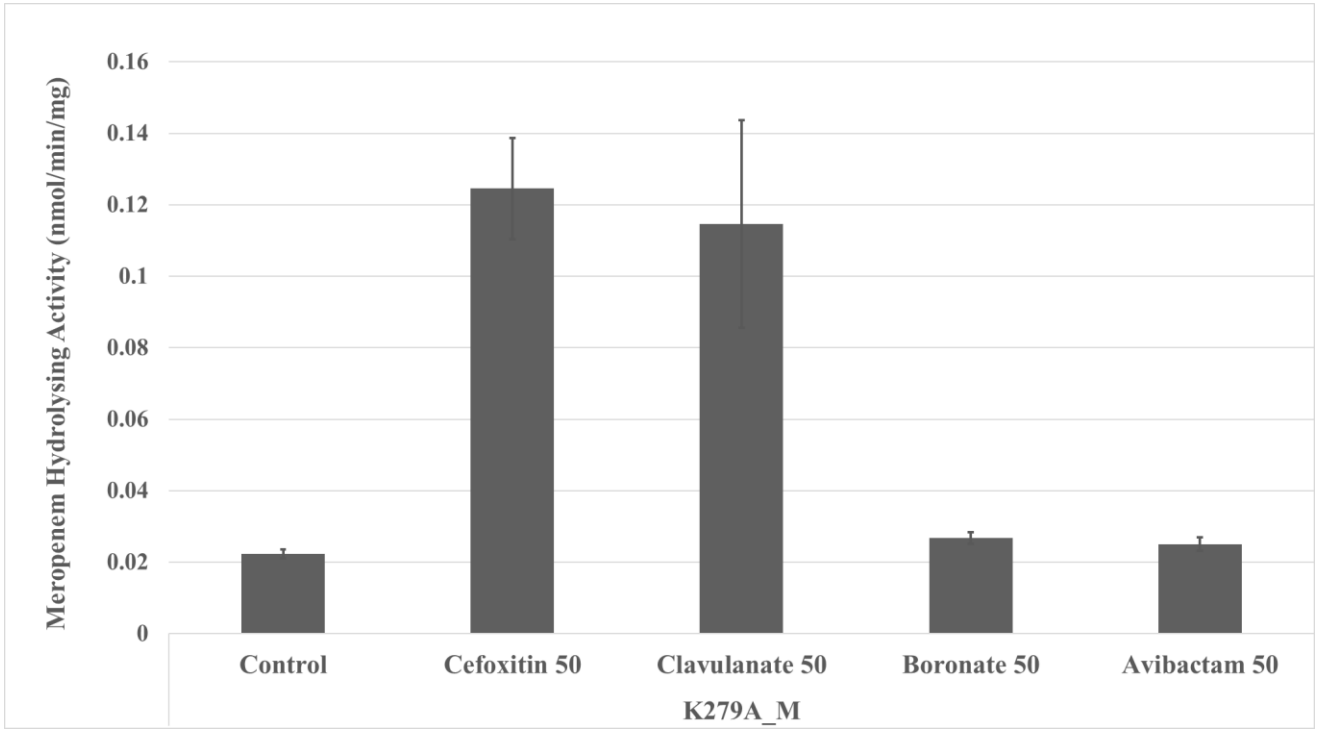
Meropenem Hydrolysing Activity (nmol/min/mg)
0.16
0.14
0.12
0.1
0.08
0.06
0.04
0.02
0
Control
Cefoxitin 50
Clavulanate 50
Boronate 50
Avibactam 50
K279A_M

Figure 7

A

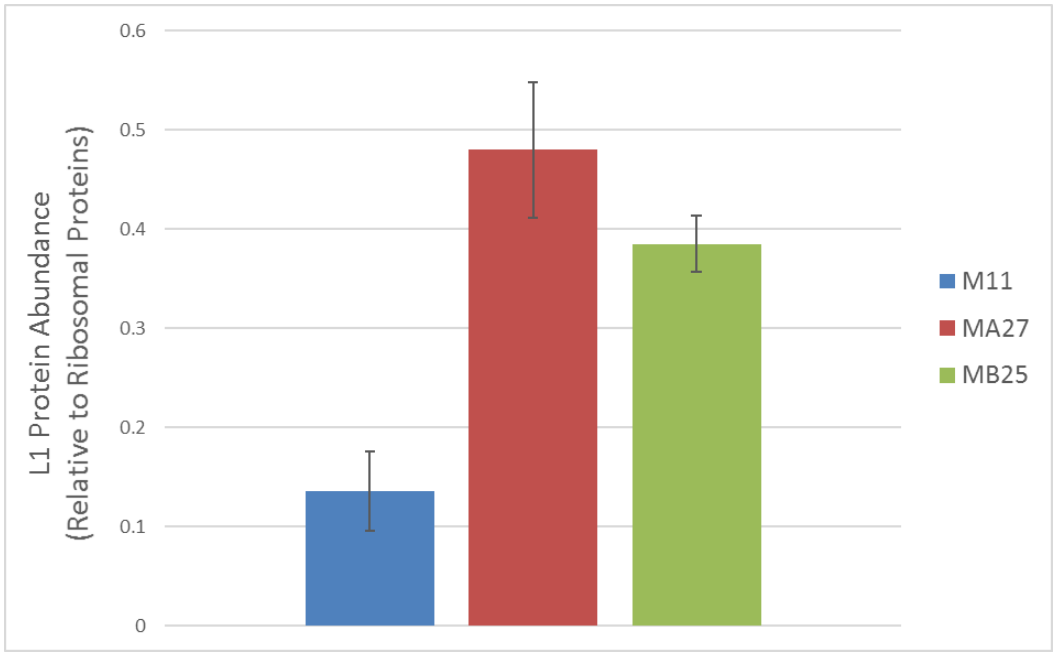
L1 Protein Abundance
(Relative to Ribosomal Proteins)
0.6
0.5
0.4
0.3
0.2
0.1
0
M11
MA27
MB25

B

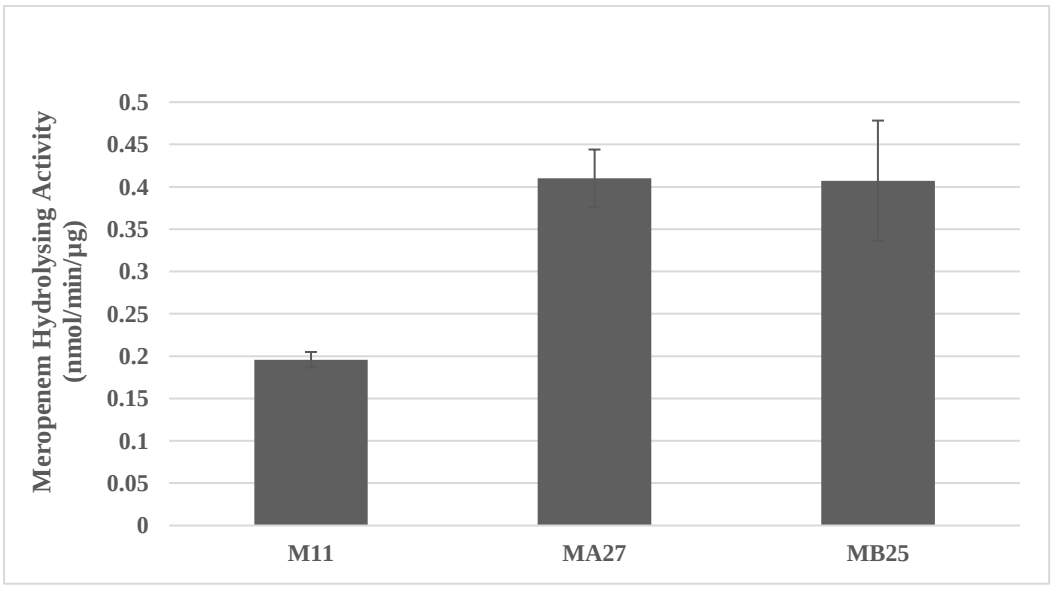
Meropenem Hydrolysing Activity
(nmol/min/µg)
0.5
0.45
0.4
0.35
0.3
0.25
0.2
0.15
0.1
0.05
0
M11
MA27
MB25

607 **Figure 8**

608

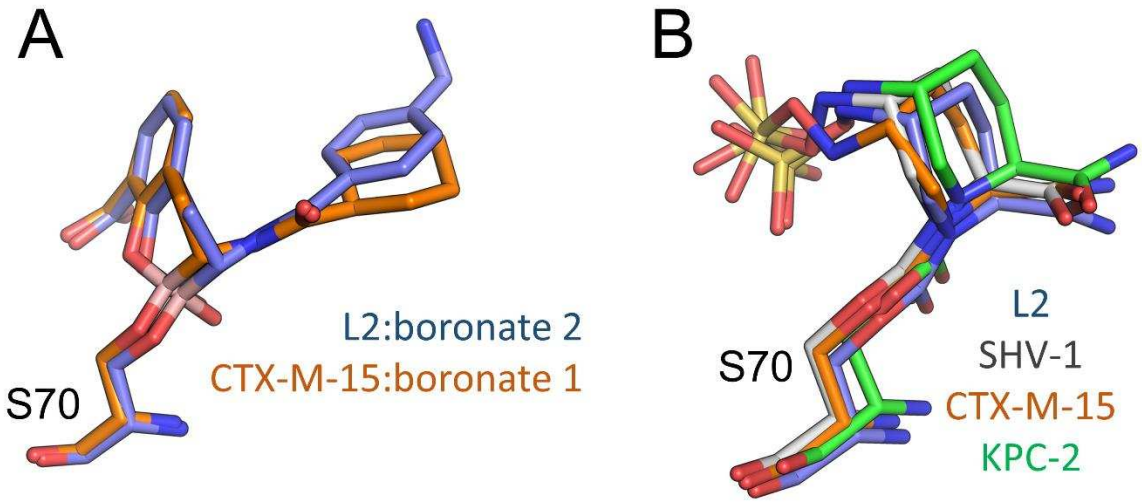

609

610 **TABLES**

611

612 **Table 1, Kinetic data for β-lactams tested against metallo L1 and serine L2 S.**

613 **maltophilia β-lactamases.**

Enzyme	Substrate	[E] (µM)	Km (µM)	k_{cat} (s^{-1})	k_{cat}/Km ($\mu M^{-1}.s^{-1}$) x10^{-3}
L1	Ceftazidime	0.5	259.5	1.67	6.4
	Aztreonam	0.5	-	-	-
	Meropenem	10	105	23.8	227
	FC5	0.05	29.6	146	4,932
L2	Ceftazidime	0.5	548.5	1.88	3.4
	Aztreonam	0.5	119.4	0.08	0.67
	Meropenem	0.625	28.83	0.028	0.97
	FC5	0.05	17.9	208.6	11,653

614

Table 2. Minimum Inhibitory Concentrations (mg/L) of β-lactams against S. maltophilia in the presence of β-lactamase inhibitors used at 2 mg/L.

	Ceftazidime				Aztreonam				Meropenem			
	-	+CLA	+BOR	+AVI	-	+CLA	+BOR	+AVI	-	+CLA	+BOR	+AVI
K279a	4	4	0.5	1	128	1	1	1	8	32	4	16
CI-20	16	16	2	4	128	4	2	2	64	32	8	64
CI-29	8	4	0.5	1	128	1	1	1	32	16	8	32
K CAZ 10	64	8	4	8	256	0.5	1	1	64	8	16	64
CI-31	256	128	128	128	256	2	4	4	256	256	256	256
K AMI 32	2	1	1	0.5	128	0.5	1	0.5	4	8	4	16
K MOX 8	4	1	0.5	0.5	128	0.25	1	0.5	4	8	8	16

Shaded values indicate clinically relevant resistance according to CLSI breakpoints (53)

CLA, clavulanic acid; BOR, bicyclic boronate **2**; AVI, avibactam

620 **Table 3. Inhibition of L2 by β-lactamase inhibitors in vitro.**

621

Inhibitor	**IC_{50} (nM)**	**pIC_{50}**
Clavulanic Acid	22.3	7.41
Avibactam	14.36	7.84
Bicyclic Boronate **2**	5.25	8.27

622

Table 4. MICs (mg/L) of β-lactams against S. maltophilia mutants in the presence of β-lactamase inhibitor (10 mg/L).

	Ceftazidime			Aztreonam		
	-	+BOR	+AVI	-	+BOR	+AVI
K279a	4	0.5	1	128	1	1
M11	128	8	2	256	1	1
MA27	256	32	32	256	4	4
MB25	256	64	128	256	4	4

Shaded values represent resistance according to CLSI breakpoints.

BOR, bicyclic boronate **2**; AVI, avibactam.

MA27 and MB25 were selected for growth at 32 mg/L ceftazidime in the presence of 10 mg/L avibactam or bicyclic boronate **2**, respectively using M11 as parent strain. M11 is an L1/L2 hyper-producing mutant derived from K279a, which is wild-type [37].

REFERENCES

1. **Hamad B.** 2010. The antibiotics market. Nat Rev Drug Discov **9:**675-676.
2. **Van Boeckel TP, Gandra S, Ashok A, Caudron Q, Grenfell BT, Levin SA, Laxminarayan R.** Global antibiotic consumption 2000 to 2010: an analysis of national pharmaceutical sales data. The Lancet Infectious Diseases **14:**742-750.
3. **Versporten A, Bolokhovets G, Ghazaryan L, Abilova V, Pyshnik G, Spasojevic T, Korinteli I, Raka L, Kambaralieva B, Cizmovic L, Carp A, Radonjic V, Maqsudova N, Celik HD, Payerl-Pal M, Pedersen HB, Sautenkova N, Goossens H, Grp WE-EP.** 2014. Antibiotic use in eastern Europe: a cross-national database study in coordination with the WHO Regional Office for Europe. Lancet Infectious Diseases **14:**381-387.
4. **Strynadka NCJ, Adachi H, Jensen SE, Johns K, Sielecki A, Betzel C, Sutoh K, James MNG.** 1992. Molecular structure of the acyl-enzyme intermediate in β-lactam hydrolysis at 1.7 A resolution. Nature **359:**700-705.
5. **Drawz SM, Bonomo RA.** 2010. Three Decades of β-Lactamase Inhibitors. Clinical Microbiology Reviews **23:**160-201.
6. **Ambler RP.** 1980. The Structure of β-Lactamases. Philosophical Transactions of the Royal Society of London B, Biological Sciences **289:**321.
7. **Bush K.** 2013. The ABCD's of β-lactamase nomenclature. Journal of Infection and Chemotherapy **19:**549-559.
8. **King AM, King DT, French S, Brouillette E, Asli A, Alexander JAN, Vuckovic M, Maiti SN, Parr TR, Brown ED, Malouin F, Strynadka NCJ, Wright GD.** 2016. Structural and Kinetic Characterization of Diazabicyclooctanes as Dual Inhibitors of Both Serine-β-Lactamases and Penicillin-Binding Proteins. ACS Chemical Biology **11:**864-868.
9. **Brem J, Cain R, Cahill S, McDonough MA, Clifton IJ, Jimenez-Castellanos JC, Avison MB, Spencer J, Fishwick CWG, Schofield CJ.** 2016. Structural basis of metallo-beta-lactamase, serine-beta-lactamase and penicillin-binding protein inhibition by cyclic boronates. Nature Communications **7**.

10. **Drawz SM, Papp-Wallace KM, Bonomo RA.** 2014. New β-Lactamase Inhibitors: a Therapeutic Renaissance in an MDR World. Antimicrobial Agents and Chemotherapy **58:**1835-1846.

11. **Al Roomi LG, Sutton AM, Cockburn F, McAllister TA.** 1984. Amoxycillin and clavulanic acid in the treatment of urinary infection. Archives of Disease in Childhood **59:**256-259.

12. **Reading C, Cole M.** 1977. Clavulanic Acid: a Beta-Lactamase-Inhibiting Beta-Lactam from Streptomyces clavuligerus. Antimicrobial Agents and Chemotherapy **11:**852-857.

13. **Fass RJ, Prior RB.** 1989. Comparative in vitro activities of piperacillin-tazobactam and ticarcillin-clavulanate. Antimicrobial Agents and Chemotherapy **33:**1268-1274.

14. **Finlay J, Miller L, Poupard JA.** 2003. A review of the antimicrobial activity of clavulanate. Journal of Antimicrobial Chemotherapy **52:**18-23.

15. **Sulton D, Pagan-Rodriguez D, Zhou X, Liu YD, Hujer AM, Bethel CR, Helfand MS, Thomson JM, Anderson VE, Buynak JD, Ng LM, Bonomo RA.** 2005. Clavulanic acid inactivation of SHV-1 and the inhibitor-resistant S130G SHV-1 beta-lactamase - Insights into the mechanism of inhibition. Journal of Biological Chemistry **280:**35528-35536.

16. **Ehmann DE, Jahić H, Ross PL, Gu R-F, Hu J, Kern G, Walkup GK, Fisher SL.** 2012. Avibactam is a covalent, reversible, non–β-lactam β-lactamase inhibitor. Proceedings of the National Academy of Sciences **109:**11663-11668.

17. **Stachyra T, Pechereau MC, Bruneau JM, Claudon M, Frere JM, Miossec C, Coleman K, Black MT.** 2010. Mechanistic studies of the inactivation of TEM-1 and P99 by NXL104, a novel non-beta-lactam beta-lactamase inhibitor. Antimicrob Agents Chemother **54:**5132-5138.

18. **Coleman K.** 2011. Diazabicyclooctanes (DBOs): a potent new class of non-β-lactam β-lactamase inhibitors. Current Opinion in Microbiology **14:**550-555.

19. **Wang DY, Abboud MI, Markoulides MS, Brem J, Schofield CJ.** 2016. The road to avibactam: the first clinically useful non-beta-lactam working somewhat like a β-lactam. Future Medicinal Chemistry **8:**1063-1084.

20. **Choi H, Paton RS, Park H, Schofield CJ.** 2016. Investigations on recyclisation and hydrolysis in avibactam mediated serine β-lactamase inhibition. Organic & Biomolecular Chemistry **14:**4116-4128.

21. **Abboud MI, Damblon C, Brem J, Smargiasso N, Mercuri P, Gilbert B, Rydzik AM, Claridge TDW, Schofield CJ, Frere JM.** 2016. Interaction of Avibactam with Class B Metallo-beta-Lactamases. Antimicrobial Agents and Chemotherapy **60:**5655-5662.

22. **Hecker SJ, Reddy KR, Totrov M, Hirst GC, Lomovskaya O, Griffith DC, King P, Tsivkovski R, Sun D, Sabet M, Tarazi Z, Clifton MC, Atkins K, Raymond A, Potts KT, Abendroth J, Boyer SH, Loutit JS, Morgan EE, Durso S, Dudley MN.** 2015. Discovery of a Cyclic Boronic Acid β-Lactamase Inhibitor (RPX7009) with Utility vs Class A Serine Carbapenemases. Journal of Medicinal Chemistry **58:**3682-3692.

23. **Cahill ST, Cain R, Wang DY, Lohans CT, Wareham DW, Oswin HP, Mohammed J, Spencer J, Fishwick CW, McDonough MA, Schofield CJ, Brem J.** 2017. Cyclic Boronates Inhibit All Classes of beta-Lactamase. Antimicrob Agents Chemother doi:10.1128/AAC.02260-16.

24. **VenatoRx Pharmaceuticals.** 2016. VNRX-5133-101/102: A Randomized, Double Blind, Placebo-Controlled, Sequential Group, Dose-Escalation Study to Evaluate the Safety, Tolerability, and Pharmacokinetics of Single and Repeat Doses of VNRX-5133 in Healthy Adult Volunteers, November 9, 2016 ed.

25. **Ryan RP, Monchy S, Cardinale M, Taghavi S, Crossman L, Avison MB, Berg G, van der Lelie D, Dow JM.** 2009. The versatility and adaptation of bacteria from the genus Stenotrophomonas. Nat Rev Micro **7:**514-525.

26. **Brooke JS.** 2012. Stenotrophomonas maltophilia: an Emerging Global Opportunistic Pathogen. Clinical Microbiology Reviews **25:**2-41.

27. **de Vrankrijker AMM, Wolfs TFW, van der Ent CK.** 2010. Challenging and emerging pathogens in cystic fibrosis. Paediatric Respiratory Reviews **11:**246-254.

712 28. **Alonso A, Martinez JL.** 2000. Cloning and characterization of SmeDEF, a novel multidrug
713 efflux pump from Stenotrophomonas maltophilia. Antimicrob Agents Chemother **44:**3079-
714 3086.
715 29. **Gould VC, Avison MB.** 2006. SmeDEF-mediated antimicrobial drug resistance in
716 Stenotrophomonas maltophilia clinical isolates having defined phylogenetic relationships. J
717 Antimicrob Chemother **57:**1070-1076.
718 30. **Garcia-Leon G, Puig CRD, de la Fuente CG, Martinez-Martinez L, Martinez JL, Sanchez**
719 **MB.** 2015. High-level quinolone resistance is associated with the overexpression of smeVWX
720 in Stenotrophomonas maltophilia clinical isolates. Clinical Microbiology and Infection **21:**464-
721 467.
722 31. **Gould VC, Okazaki A, Avison MB.** 2013. Coordinate hyperproduction of SmeZ and SmeJK
723 efflux pumps extends drug resistance in Stenotrophomonas maltophilia. Antimicrob Agents
724 Chemother **57:**655-657.
725 32. **Walsh TR, Hall L, Assinder SJ, Nichols WW, Cartwright SJ, Macgowan AP, Bennett PM.**
726 1994. Sequence-Analysis of the L1 Metallo-Beta-Lactamase from Xanthomonas-Maltophilia.
727 Biochimica Et Biophysica Acta-Gene Structure and Expression **1218:**199-201.
728 33. **Walsh TR, MacGowan AP, Bennett PM.** 1997. Sequence analysis and enzyme kinetics of
729 the L2 serine beta-lactamase from Stenotrophomonas maltophilia. Antimicrobial Agents and
730 Chemotherapy **41:**1460-1464.
731 34. **Gould VC, Okazaki A, Avison MB.** 2006. Beta-lactam resistance and beta-lactamase
732 expression in clinical Stenotrophomonas maltophilia isolates having defined phylogenetic
733 relationships. J Antimicrob Chemother **57:**199-203.
734 35. **Lemmen SW, Häfner H, Reinert RR, Zolldann D, Kümmerer K, Lütticken R.** 2001.
735 Comparison of serum bactericidal activity of ceftazidime, ciprofloxacin and meropenem
736 against Stenotrophomonas maltophilia. Journal of Antimicrobial Chemotherapy **47:**118-120.
737 36. **Okazaki A, Avison MB.** 2008. Induction of L1 and L2 beta-lactamase production in
738 Stenotrophomonas maltophilia is dependent on an AmpR-type regulator. Antimicrob Agents
739 Chemother **52:**1525-1528.

37. **Talfan A, Mounsey O, Charman M, Townsend E, Avison MB.** 2013. Involvement of mutation in ampD I, mrcA, and at least one additional gene in beta-lactamase hyperproduction in Stenotrophomonas maltophilia. Antimicrob Agents Chemother **57:**5486-5491.

38. **Crossman LC, Gould VC, Dow JM, Vernikos GS, Okazaki A, Sebaihia M, Saunders D, Arrowsmith C, Carver T, Peters N, Adlem E, Kerhornou A, Lord A, Murphy L, Seeger K, Squares R, Rutter S, Quail MA, Rajandream M-A, Harris D, Churcher C, Bentley SD, Parkhill J, Thomson NR, Avison MB.** 2008. The complete genome, comparative and functional analysis of Stenotrophomonas maltophilia reveals an organism heavily shielded by drug resistance determinants. Genome Biology **9:**R74-R74.

39. **Huang YW, Lin CW, Ning HC, Lin YT, Chang YC, Yang TC.** 2017. Overexpression of SmeDEF Efflux Pump Decreases Aminoglycoside Resistance in Stenotrophomonas maltophilia. Antimicrob Agents Chemother doi:10.1128/AAC.02685-16.

40. **van Berkel SS, Brem J, Rydzik AM, Salimraj R, Cain R, Verma A, Owens RJ, Fishwick CWG, Spencer J, Schofield CJ.** 2013. Assay Platform for Clinically Relevant Metallo-β-lactamases. Journal of Medicinal Chemistry **56:**6945-6953.

41. **Meroueh SO, Fisher JF, Schlegel HB, Mobashery S.** 2005. Ab Initio QM/MM Study of Class A β-Lactamase Acylation: Dual Participation of Glu166 and Lys73 in a Concerted Base Promotion of Ser70. Journal of the American Chemical Society **127:**15397-15407.

42. **Fonseca F, Chudyk EI, van der Kamp MW, Correia A, Mulholland AJ, Spencer J.** 2012. The Basis for Carbapenem Hydrolysis by Class A β-Lactamases: A Combined Investigation using Crystallography and Simulations. Journal of the American Chemical Society **134:**18275-18285.

43. **Vandavasi VG, Weiss KL, Cooper JB, Erskine PT, Tomanicek SJ, Ostermann A, Schrader TE, Ginell SL, Coates L.** 2016. Exploring the Mechanism of β-Lactam Ring Protonation in the Class A β-lactamase Acylation Mechanism Using Neutron and X-ray Crystallography. Journal of Medicinal Chemistry **59:**474-479.

44. **Hanes MS, Jude KM, Berger JM, Bonomo RA, Handel TM.** 2009. Structural and Biochemical Characterization of the Interaction between KPC-2 β-Lactamase and β-Lactamase Inhibitor Protein. Biochemistry **48:**9185-9193.

45. **Krishnan NP, Nguyen NQ, Papp-Wallace KM, Bonomo RA, van den Akker F.** 2015. Inhibition of Klebsiella beta-Lactamases (SHV-1 and KPC-2) by Avibactam: A Structural Study. Plos One **10**.

46. **King DT, King AM, Lal SM, Wright GD, Strynadka NCJ.** 2015. Molecular Mechanism of Avibactam-Mediated beta-Lactamase Inhibition. Acs Infectious Diseases **1:**175-184.

47. **Lahiri SD, Mangani S, Jahic H, Benvenuti M, Durand-Reville TF, De Luca F, Ehmann DE, Rossolini GM, Alm RA, Docquier JD.** 2015. Molecular Basis of Selective Inhibition and Slow Reversibility of Avibactam against Class D Carbapenemases: A Structure-Guided Study of OXA-24 and OXA-48. Acs Chemical Biology **10:**591-600.

48. **Xu H, Hazra S, Blanchard JS.** 2012. NXL104 Irreversibly Inhibits the beta-Lactamase from Mycobacterium tuberculosis. Biochemistry **51:**4551-4557.

49. **Lahiri SD, Mangani S, Durand-Reville T, Benvenuti M, De Luca F, Sanyal G, Docquier JD.** 2013. Structural Insight into Potent Broad-Spectrum Inhibition with Reversible Recyclization Mechanism: Avibactam in Complex with CTX-M-15 and Pseudomonas aeruginosa AmpC beta-Lactamases. Antimicrobial Agents and Chemotherapy **57:**2496-2505.

50. **Lahiri SD, Johnstone MR, Ross PL, McLaughlin RE, Olivier NB, Alm RA.** 2014. Avibactam and Class C beta-Lactamases: Mechanism of Inhibition, Conservation of the Binding Pocket, and Implications for Resistance. Antimicrobial Agents and Chemotherapy **58:**5704-5713.

51. **Jacobs C, Frère J-M, Normark S.** 1997. Cytosolic Intermediates for Cell Wall Biosynthesis and Degradation Control Inducible β-Lactam Resistance in Gram-Negative Bacteria. Cell **88:**823-832.

52. **Jacobs C, Huang LJ, Bartowsky E, Normark S, Park JT.** 1994. Bacterial cell wall recycling provides cytosolic muropeptides as effectors for beta-lactamase induction. The EMBO Journal **13:**4684-4694.

53. **CLSI.** 2015. Performance Standards for Antimicrobial Susceptibility Testing; Twenty-Fifth Informational Supplement. Wayne, PA: Clinical and Laboratory Standards Institute **CLSI document M100-S25**.

54. **Stachyra T, Levasseur P, Péchereau M-C, Girard A-M, Claudon M, Miossec C, Black MT.** 2009. In vitro activity of the β-lactamase inhibitor NXL104 against KPC-2 carbapenemase and Enterobacteriaceae expressing KPC carbapenemases. Journal of Antimicrobial Chemotherapy **64:**326-329.

55. **Mojica MF, Ouellette CP, Leber A, Becknell MB, Ardura MI, Perez F, Shimamura M, Bonomo RA, Aitken SL, Shelburne SA.** 2016. Successful Treatment of Bloodstream Infection Due to Metallo-β-Lactamase-Producing Stenotrophomonas maltophilia in a Renal Transplant Patient. Antimicrobial Agents and Chemotherapy **60:**5130-5134.

56. **Blizzard TA, Chen H, Kim S, Wu J, Bodner R, Gude C, Imbriglio J, Young K, Park Y-W, Ogawa A, Raghoobar S, Hairston N, Painter RE, Wisniewski D, Scapin G, Fitzgerald P, Sharma N, Lu J, Ha S, Hermes J, Hammond ML.** 2014. Discovery of MK-7655, a β-lactamase inhibitor for combination with Primaxin®. Bioorganic & Medicinal Chemistry Letters **24:**780-785.

57. **Burns CJ, Goswami R, Jackson RW, Lessen T, Li W, Pevear D, Tirunahari PK, Xu H.** 2010. Beta-lactamase inhibitors. Google Patents.

58. **Silva JC, Gorenstein MV, Li GZ, Vissers JP, Geromanos SJ.** 2006. Absolute quantification of proteins by LCMSE: a virtue of parallel MS acquisition. Mol Cell Proteomics **5:**144-156.

59. **Calvopina K, Umland KD, Rydzik AM, Hinchliffe P, Brem J, Spencer J, Schofield CJ, Avison MB.** 2016. Sideromimic Modification of Lactivicin Dramatically Increases Potency against Extensively Drug-Resistant Stenotrophomonas maltophilia Clinical Isolates. Antimicrob Agents Chemother **60:**4170-4175.

60. **Gorrec F.** 2009. The MORPHEUS protein crystallization screen. Journal of Applied Crystallography **42:**1035-1042.

61. **Kabsch W.** 2010. XDS. Acta Crystallographica Section D **66:**125-132.

62. **Waterman DG, Winter G, Gildea RJ, Parkhurst JM, Brewster AS, Sauter NK, Evans G.** 2016. Diffraction-geometry refinement in the DIALS framework. Acta Crystallographica Section D **72:**558-575.

63. **Winn MD, Ballard CC, Cowtan KD, Dodson EJ, Emsley P, Evans PR, Keegan RM, Krissinel EB, Leslie AGW, McCoy A, McNicholas SJ, Murshudov GN, Pannu NS, Potterton EA, Powell HR, Read RJ, Vagin A, Wilson KS.** 2011. Overview of the CCP4 suite and current developments. Acta Crystallographica Section D: Biological Crystallography **67:**235-242.

64. **McCoy AJ, Grosse-Kunstleve RW, Adams PD, Winn MD, Storoni LC, Read RJ.** 2007. Phaser crystallographic software. Journal of Applied Crystallography **40:**658-674.

65. **Moriarty NW, Grosse-Kunstleve RW, Adams PD.** 2009. electronic Ligand Builder and Optimization Workbench (eLBOW): a tool for ligand coordinate and restraint generation. Acta Crystallographica Section D **65:**1074-1080.

66. **Emsley P, Lohkamp B, Scott WG, Cowtan K.** 2010. Features and development of Coot. Acta Crystallographica Section D **66:**486-501.

67. **Adams PD, Afonine PV, Bunkoczi G, Chen VB, Davis IW, Echols N, Headd JJ, Hung L-W, Kapral GJ, Grosse-Kunstleve RW, McCoy AJ, Moriarty NW, Oeffner R, Read RJ, Richardson DC, Richardson JS, Terwilliger TC, Zwart PH.** 2010. PHENIX: a comprehensive Python-based system for macromolecular structure solution. Acta Crystallographica Section D **66:**213-221.

68. **Chen VB, Arendall WB, III, Headd JJ, Keedy DA, Immormino RM, Kapral GJ, Murray LW, Richardson JS, Richardson DC.** 2010. MolProbity: all-atom structure validation for macromolecular crystallography. Acta Crystallographica Section D **66:**12-21.